Laboratory testing of steel fibre reinforced shotcrete.

H. Saw[*], E. Villaescusa, C.R. Windsor and A.G. Thompson

CRC Mining, Western Australian School of Mines, Curtin University of Technology, PMB 22, Kalgoorlie 6430, Australia

Abstract

Uniaxial and triaxial compression tests on steel fibre reinforced shotcrete (SFRS) have been used to quantify elastic-plastic response behaviour for both the peak and post-peak regions. The laboratory tests were conducted with a servo-controlled testing machine to obtain complete stress-strain curves. The test results include unconfined and triaxial compressive strength, shear strength and tensile strength together with the elastic and plastic mechanical properties of SFRS. A method is also suggested for obtaining the plasticity parameters for non-linear modeling of SFRS.

Keywords: Uniaxial and triaxial compression tests, Steel fibre reinforced shotcrete, elastic and plastic mechanical properties.

[*] Corresponding author. Tel.: +61-8-90886099 fax: +61-8-90886151 Email: h.saw@curtin.edu.au

1. Introduction

The theory of plasticity is the name given to the mathematical study of stress and strain in plastically deformed solids [1]. Hill published the book "Mathematical theory of plasticity" based mainly on the test results of metals. However, he did suggest that the theory may apply to other potentially plastic materials. Since that time, extensive research and development has been conducted on the application of plasticity theory to other materials such as soils, rocks, concrete and shotcrete. To date, the theory has reached a good degree of maturity for application to geomaterials, although further progress is still expected [2]. At the same time the continual development of testing equipment, computing methods, software and hardware enhance the application of plasticity theory.

Shotcrete is a designed material with anisotropic, inhomogeneous and elastic-plastic behaviour. Therefore, understanding of the complete stress-strain behavior of shotcrete is extremely important in ground support design; especially in cases where large deformations are expected such as around mine excavations at great depth. A rock mass is naturally Discontinuous, Inhomogeneous, Anisotropic, and Non-Elastic (DIANE), [3]. When a rock mass deforming non-linearly, the shotcrete also responds non-linearly. Deformation mechanisms of shotcrete which support the rock mass surface excavated by drill and blast methods are described by Windsor and Thompson [4].

2. Literature review and objectives of study

Tejchman and Kozicki [5] review the works of different researches on the steel fibre reinforced concrete and summarised the most important physical and mechanical properties of steel fibres reinforced concrete/shotcrete. Most of the experiments were concerned with the influences of constituent material such as the types and dosages of fibre, cement, aggregate, etc., on the physical and mechanical properties of steel fibre reinforced concrete/shotcrete. The

literature shows that the most common tests are uniaxial compressive strength (UCS), beam flexural strength, toughness and energy absorption test [eg. 6]. Many parameters are required for non-linear elastic-plastic numerical modeling for the rock mass and rock improvement system (rock bolts, shotcrete and wire mesh). The fundamental material parameters include; Young's modulus, Poisson's ratio, uniaxial compressive strength (UCS), shear strength (both peak and residual c and ϕ), tensile strength, dilation angle (ψ) and strain rate at peak and residual stress. In addition, account need to be taken of the geological conditions to cooperate major and minor structures, stresses and hydrology. The only parameters vary according to the models implicated with the software.

The main objectives of this study are to quantify elastic-plastic response behaviour for both the peak and post-peak regions under uniaxial and triaxial loading, to predict the shear strength in terms of cohesion, friction and dilation angle and, to examine how these parameters vary with curing time. Only the parameters directly derived from the laboratory test results are presented. The laboratory test results are presented as simple stress-strain curves. No numerical modeling was attempted to correlate with the test results. The stress-strain curves are presented as raw data.

3. A complete stress-strain relation

In the elastic region the strains are linearly related to the stress as assumed in Hooke's Law [7]. In the elastic region strains are uniquely determined by stresses and can be computed directly using Hooke's law without any regard to how the stress state was attained. Mathematically, elastic strain and stress can be simply written as:

$$\varepsilon^e = \frac{\sigma}{E} \tag{1}$$

Where, ε^e is elastic strain, σ is stress and E is Young's modulus.

In the plastic region, the strains are not uniquely determined by the stresses but depend on the whole history of loading or how the stress state was reached. An essential part of plasticity theory is to define when the material starts to deform or yield. A failure criterion is used to describe by point at which fracture or yield occurs. The criterion under which yield occurs is called a yield criterion. The most widely used yield criterion is the Coulomb yield criterion [8],

$$\tau = c + \sigma_n \tan\phi \tag{2}$$

Where, τ and σ_n represent shear stress and normal stress, respectively. Compressive stress components are treated as positive, as is usual in geomechanics. The parameters c and ϕ are assumed to be constants called the cohesion and the angle of internal friction. In reality c and ϕ change with stress level. Once the yield criterion is satisfied, the material will flow obeying the flow rule. The flow rule is termed associated if the plastic strains are associated directly with the yield surface and if not it is termed non-associated. The non-associated flow rule states that the plastic strain rate is proportional to the derivatives of the plastic potential with respect to the corresponding stress. This can be described by the following equation.

$$\dot{\varepsilon}^p = \lambda \frac{\partial g}{\partial \sigma} \tag{3}$$

where, $\dot{\varepsilon}^p$ is plastic strain increment, λ is Lagrange or plastic multiplier and g is a plastic potential. The definition of plastic potential function "g" suggested by Radenkovic [9] is,

$$g = \tau + \sigma\sin\psi + constant \tag{4}$$

where, ψ is the dilation angle. Hansen suggested, a dilation angle is defined as the ratio of plastic volume change over plastic shear strain [10].

For the Mohr-Coulomb yield criterion, equation (4) can be written in terms of principal stresses for triaxial test conditions where, $\sigma_2 = \sigma_3$,

$$g = \frac{1}{2}(\sigma_1 - \sigma_3) + \frac{1}{2}(\sigma_1 + \sigma_3)\sin\psi + constant \tag{5}$$

The principal plastic strain rates are obtained by differentiating equation (5) with respect to the principal stresses as given in equation (3).

$$\begin{bmatrix} \dot{\varepsilon}_1^p \\ \dot{\varepsilon}_2^p \\ \dot{\varepsilon}_3^p \end{bmatrix} = \lambda \begin{bmatrix} \frac{1}{2}(1 + \sin\psi) \\ \frac{1}{2}(-1 + \sin\psi) \\ \frac{1}{2}(-1 + \sin\psi) \end{bmatrix} \tag{6}$$

where, $\dot{\varepsilon}_1^p$, $\dot{\varepsilon}_2^p$ and $\dot{\varepsilon}_3^p$ are major, intermediate and minor plastic strain increment.

From which,

$$\dot{\varepsilon}_v^p = \lambda \sin\psi \tag{7}$$

$$\dot{\varepsilon}_1^p = \lambda \frac{1}{2}(1 + \sin\psi) \tag{8}$$

where, $\dot{\varepsilon}_v^p$ (volumetric strain increment) is the sum of $\dot{\varepsilon}_1^p$, $\dot{\varepsilon}_2^p$ and $\dot{\varepsilon}_3^p$.

By eliminating λ from equations (7) and (8), sin ψ is given by,

$$\sin\psi = \frac{\dot{\varepsilon}_v^p}{2\dot{\varepsilon}_1^p + \dot{\varepsilon}_v^p} \tag{9}$$

This equation for sin ψ can be expressed as,

$$\sin\psi = \frac{\dot{\varepsilon}_v^p / \dot{\varepsilon}_v^p}{2\dot{\varepsilon}_1^p / \dot{\varepsilon}_v^p + \dot{\varepsilon}_v^p / \dot{\varepsilon}_v^p} \tag{10}$$

Or

$$\sin \psi = \frac{1}{2\dot{\varepsilon}_1^p/\dot{\varepsilon}_v^p + 1} \tag{11}$$

$\dot{\varepsilon}_v^p/\dot{\varepsilon}_1^p$ give the slope of volumetric – axial strain curve. Therefore, the inverse of the slope can be substituted into equation (11) to obtain the dilation angle ψ.

The total strain, ε^t the sum of elastic and plastic strains, may written as,

$$\varepsilon^t = \varepsilon^e - \varepsilon^p \tag{12}$$

where, ε^t is total strain, ε^e is elastic strain and ε^p is plastic strain.

4. Experimental program

4.1 Mid design and curing method

The wet mix shotcrete used in these investigations is similar to that used at the one of underground gold mines in Eastern Gold Fields region, Kalgoorlie, Western Australia. Shotcrete panels were sprayed on site and delivered to the WASM geomechanics laboratory on the same day. The specimen were cored from the panels and stored in a curing chamber, which was set at 30ºC and 90% humidity. The tests were conducted on three batches of samples after at four different curing periods (1, 3, 7 and 28 days). All of the shotcrete batches have the same mix design which given in Table 1.

4.2 Test method

Both uniaxial and triaxial compressive test were conducted according to the test method suggested by International Society of Rock Mechanics (ISRM) [11, 12 & 13]. These tests were performed using an Instron, servo controlled hydraulic testing machine. The loading rate of the machine was set at 0.12 mm/min. The strains were measured with two biaxial foil strain gages with 10 mm gage length that were installed diametrically at specimen mid-height. The triaxial

compression test is a useful test method to obtain complete stress-strain response of the SFRS sample and to derive the shear strength parameters and dilation angles. Three different confining pressures 1, 2 and 3 MPa were applied to three specimens. The tensile strength was obtained according to the test method suggested by ISRM [14]. The test was performed with Avery universal testing machine. Load and displacement were monitored and stored at resolutions of 0.01kN and 0.02mm, respectively.

5. Results and discussion

5.1 Uniaxial compressive strength test results

The test results are summarised in Table 2. The stress-strain curves are shown in Figure 1. The test results show that UCS increases with curing time and that Young's modulus and Poisson's ratio do not change significantly. The yield point of the curves increased with increasing UCS. After yield, non-linear strain hardening can be observed until it reaches peak. After peak, localized damage develops and strain softening and/or the "snap-back" begins. The "snap-back" implies that the materials failed in brittle mode. Globally, the SFRS continued deforme in shear associated by dilation with the load taken by steel fibres. The effective steel fibres are which span the failure surface and are firmly anchored on both sides. The post peak behaviour of SFRS is highly dependent on the numbers and orientation of the effective fibres. Figure 2 shows that effective steel fibre with various orientations respond in different modes. The responses are predominantly shear, tensile and compression in nature. The most common response is a combination of these modes.

5.2 Indirect tensile strength test results (Brazilian method)

Similar to the UCS tests, the tensile strength also increases with curing age. The summary of Brazilian test results is given in Table 3. Figure 3 shows the load-displacement curves for indirect tensile strength tests. The results suggested that, after first crack the load is taken by the

effective fibres and the ultimate tensile strength depends on the numbers and orientation of the effective fibres. Figure 4 shows the correlation between the UCS and the peak tensile strength. The correlation suggests that the peak tensile strength of SFRS is about 15% of UCS.

5.3 Triaxial test results

A summary of test results is given in Table 4. The shear strength parameters presented in Table 4 are calculated based on Coulomb's failure theory [7 & 12]. Alternatively, the peak and residual strength envelopes plotted on the p-q plane are also shown in Figure 5 and 6 respectively. Generally, the shear strength increased with curing time. The friction and dilation angle do not change significantly with curing time. The residual strength is influenced by confining pressure. Main course of increase in strength was in increase in cohesion, the slope of the lines associated with friction angle were very similar.

The stress-strain curves shown in Figure 7 can be used to calculate the plastic strain rate at peak and residual using the total strain equation (12). The plastic strain increased with increased confining pressure. The peak stress does not change significantly from 1 day to 7 days curing but significantly increased at 28 days. The dilation angles are calculated from the axial and volumetric stain curves as described in section 3. Figures 8 shows axial and volumetric strain curves at 1 MPa confinement. The correlation of friction and dilation angle is shown in Figure 9. This suggests that, higher dilation occurred in samples with lower friction angle. Also, the amount of dilation decreases with increasing confining pressure.

6. Concluding remarks

A test programme was conducted on steel fibre reinforced shotcrete (SFRS) samples to define the mechanical parameters for non-linear, elastic-plastic modelling. In particular, uniaxial and triaxial compression tests and Brazilian tests have been used to quantify elastic-plastic response behaviour for

both the pre-peak and post-peak regions. The findings suggested that, the residual strength is influenced by the confining pressure as the specimen responded in continuously strain hardening after post peak. The dilation angle ranges from 8 to 13 degrees and does not change significantly with curing time. It decreases with increasing friction angle. The amount of dilation decrease with increasing confining pressure. A complete stress-strain response can be subdivided into linear elastic and non-linear plastic regions. The non-liner plastic region includes strain hardening up to the post peak (which plateau at high confining pressure), snap-back or/and strain softening after post peak. A snap-back occurs when the SFRS responds locally in the brittle mode. The post peak behavior is influenced by the confining pressure and the number and orientation of effective fibres.

Acknowledgements

References

1. Hill R. The Mathematical Theory of Plasticity. Oxford, University Press; 1950.

2.   Yu HS. Plasticity and Geotechnics. New York, Springer Science and Business Media; 2006.

3. Harrison JP & Hudson JA. Engineering Rock Mechanics: Part 2, Oxford, Elsevier; 2000.

4. Windsor CR & Thompson AG (1999). The design of shotcrete linings for excavations created by drill and blast methods. In: Proceeding of international symposium on ground support. Kalgoorlie; 1999. p. 231-41.

5. Jacek T & Jan K. Experimental and theoretical investigation of steel-fibrous concrete. Verlag Berlin Heidelberg, Springer;2010.

6. Morgan DR. et al. Fibre reinforced shotcrete. In: Shotcrete - A compilation of papers, DR Morgan, Farmington Hill: American Shotcrete Association, 2008. Pp. 95-191.

7. Hooke R. The posthumous Works, Containing his Cutlerian Lectures, and other Discourses. Read at the Meeting of the Illustrious Royal Society; 1705.

8. Coulomb C A. Essais sur une application des regles des maximis et minimis à quelques problems de statique relatifs à l'architecture. Mem. Acad; 1776.

9. Radenkovic D. Théorèmes limites pour un matériau de Coulomb á dilation non standardisée. C.R. Ac.Sc. 252, Paris; 1961. pp. 4103-04.

10. Hansen CEB. Line ruptures regarded as narrow rupture zones - Basic equations based on kinematic considerations. In proceeding of conference on Earth Pressure Problem, Brussels; 1958.

11. ISRM. Suggested methods for determining the uniaxial compressive strength and deformability of rock material. In: Brown ET editor. Rock characterization, testing and monitoring: ISRM suggested Methods. Oxford: Pergamon; 1981.p. 137–40.

12. Fairhurst C E & Hudson J A. Draft ISRM suggested method for the complete stress-strain curve for intact rock in uniaxial compression. Int J Rock Mech Min Sci 1999;36:279- 89.

13. ISRM. Suggested methods for determining the strength of rock materials in triaxial compression: revised version. Int J Rock Mech Min Sci 1983;20:285-90.

14. ISRM. Suggested methods for determining tensile strength of rock mateials. Int J Rock Mech Min Sci 1978;15:90-103.

APPENDIX

Table 1. Mix design of SFRS used in this research.

Material	Quantity for 1 m³ mix
Cement (GP)	400 kg
Coarse aggregate (7-10 mm)	220 kg
Crusher dust	1300 kg
Sand	1640 kg
Water	150 L
Steel fibres	30 kg
Liquid Meyco (MS 685)	11 L
Delvo Stabiliser	5 L
Rheobuild 1000	8 L
Pozzolith 322Ni	1.3 L
Accelerator	4% of cement

Table 2. Summary of UCS test with complete stress-strain measurement.

Batch No.	Curing (Days)	Unit weight (kN/m³)	UCS σ_c (MPa)	Elastic properties					
				Young's modulus			Poisson's ratio		
				E_{t50} (GPa)	E_s (GPa)	E_a (GPa)	ν_{t50}	ν_s	ν_a
1	1	20.71	16.2	-	-	-	-	-	-
2	1	20.71	18.1	14	15	14	0.36	0.31	0.42
3	1	23.44	18.3	11	16	11	0.20	0.28	0.19
1	3	23.44	23.4	-	-	-	-	-	-
2	3	22.75	18.3	12	15	12	0.28	0.29	0.28
3	3	23.39	22.9	9	13	8	0.16	0.21	0.16
1	7	23.54	28.5	-	-	-	-	-	-
2	7	23.48	23.2	16	21	16	0.23	0.34	0.22
3	7	23.57	25.7	14	17	14	0.17	0.29	0.17
1	28	23.44	32.8	15	21	14	0.21	0.31	0.21
2	28	23.68	27.2	18	28	17	0.30	0.29	0.29
	28	23.05	31.5	11	16	10	0.17	0.22	0.15

E_{t50} = Tangent Young's modulus
E_s = Secant Young's modulus
E_a = Average Young's modulus
ν_{t50} = Tangent Poisson's ratio
ν_s = Secant Poisson's ratio
ν_a = Average Poisson's ratio

Table 4. Summary of Brazilian test results.

Batch No.	Curing (days)	Peak tensile strength (MPa)
3	1	2.4
3	1	2.5
2	3	3.4
3	3	2.8
3	3	4.3
3	3	3.5
2	7	4.4
2	7	4.0
3	7	3.6
3	7	2.8
3	7	3.2
1	28	5.5
1	28	4.0
2	28	4.9
3	28	5.4
3	28	5.1
3	28	4.8

Table 3. Summary of Triaxial test results.

Batch No.	Curing (Days)	Shear strength				Average dilation angle $\psi°$
		Peak		Residual		
		c (MPa)	$\phi°$	c (MPa)	$\phi°$	
1	1	4	38	-	-	-
2	1	4	45	2	45	8
3	1	5	36	5	32	13
1	3	5	40	3	42	-
2	3	4	40	3	41	10
3	3	6	38	-	-	12
1	7	8	35	5	35	-
2	7	5	40	4	41	10
3	7	6	40	5	38	10
1	28	8	38	7	18	12
2	28	11	18	-	-	12
3	28	8	38	-	-	10
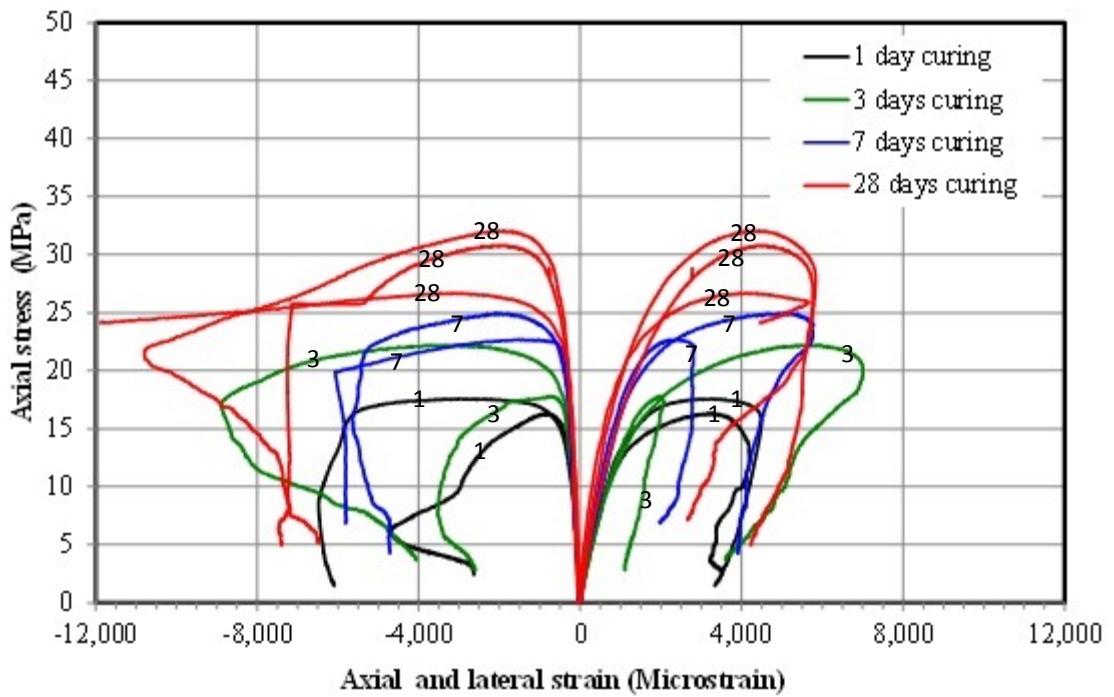
Figure 1. Stress versus strain curves from UCS test.

a=Pure shear
b=Shear + Tension
c=Tension + Shear
d=Pure tension
e=Shear + Compression
f=Compression + Shear

Shearing and dilating failure surface
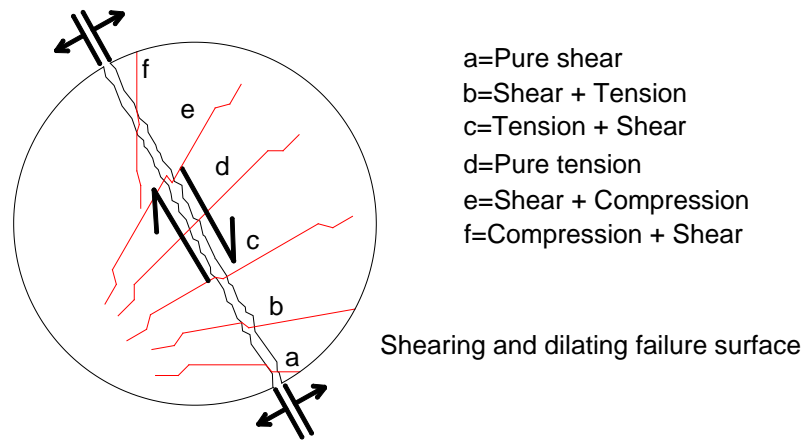
Figure 2. Effective fibre with various response modes for different fibre orientation.
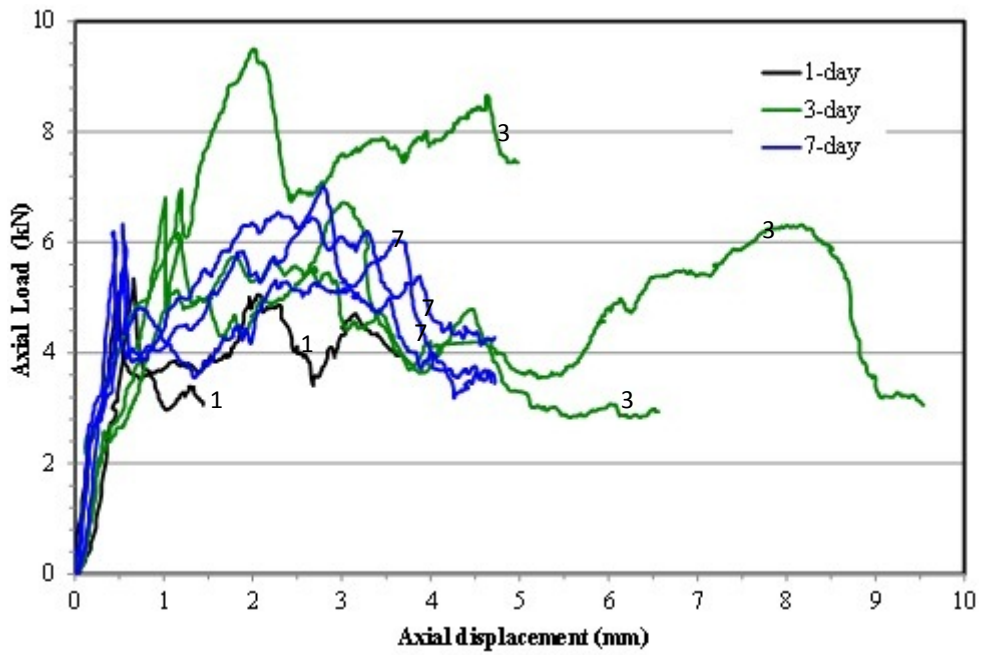(Modified from Windsor, 1996).

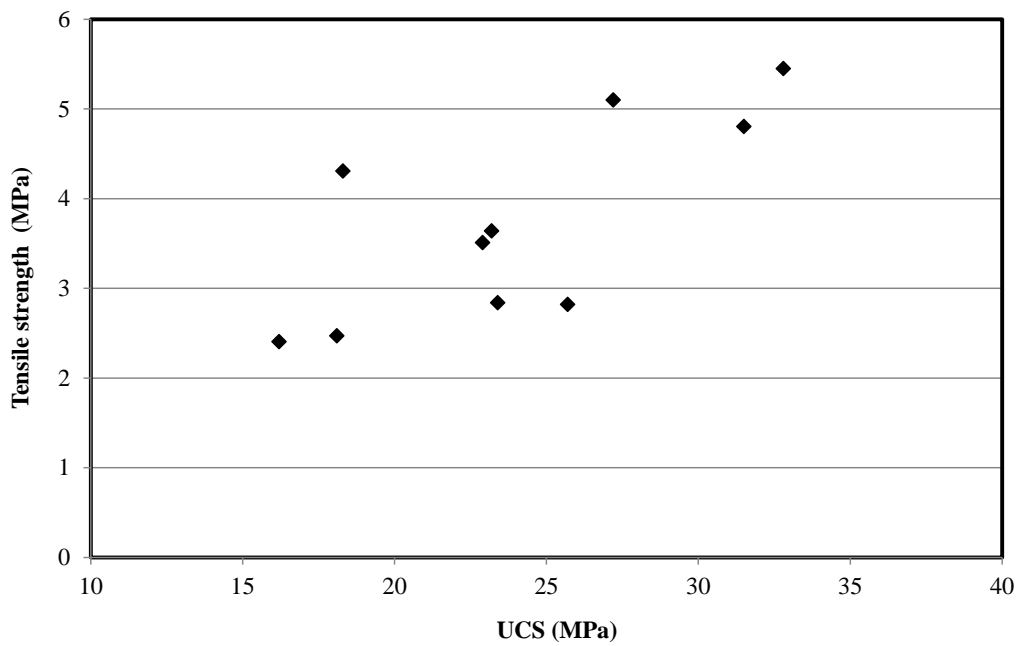Figure 3. Load-displacement curves from Brazilain tests.
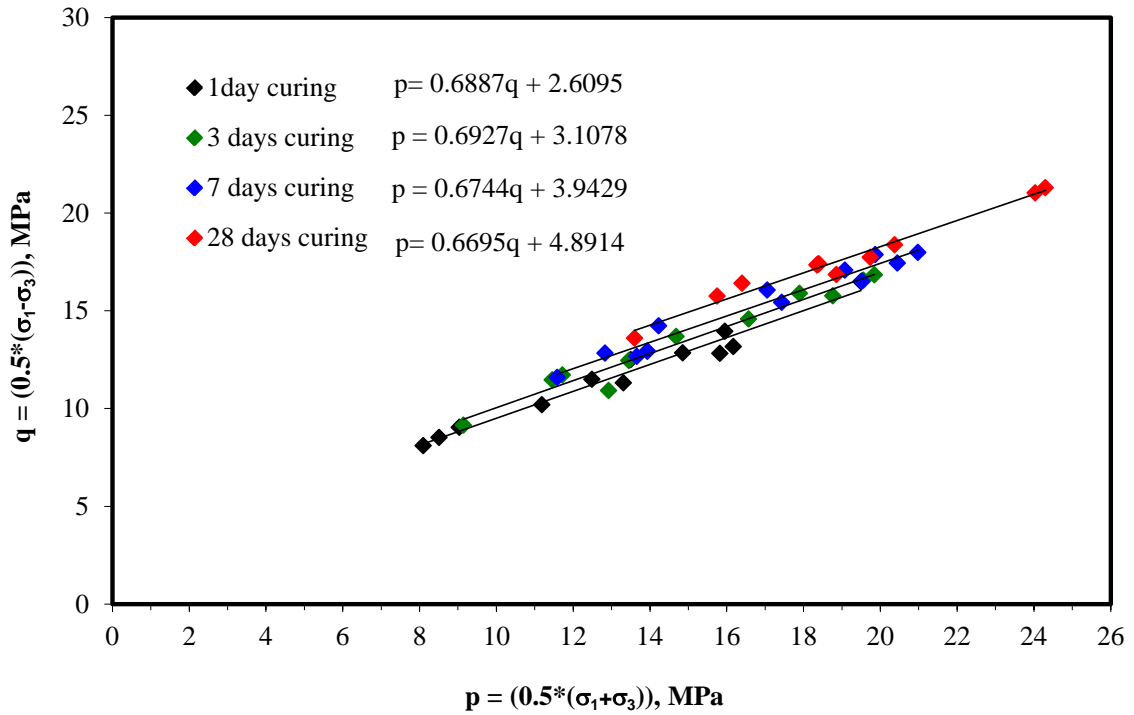

Figure 4. Correlation of peak tensile strength and UCS.

Figure 5. Peak shear strength envelopes plotted on the p-q plane.
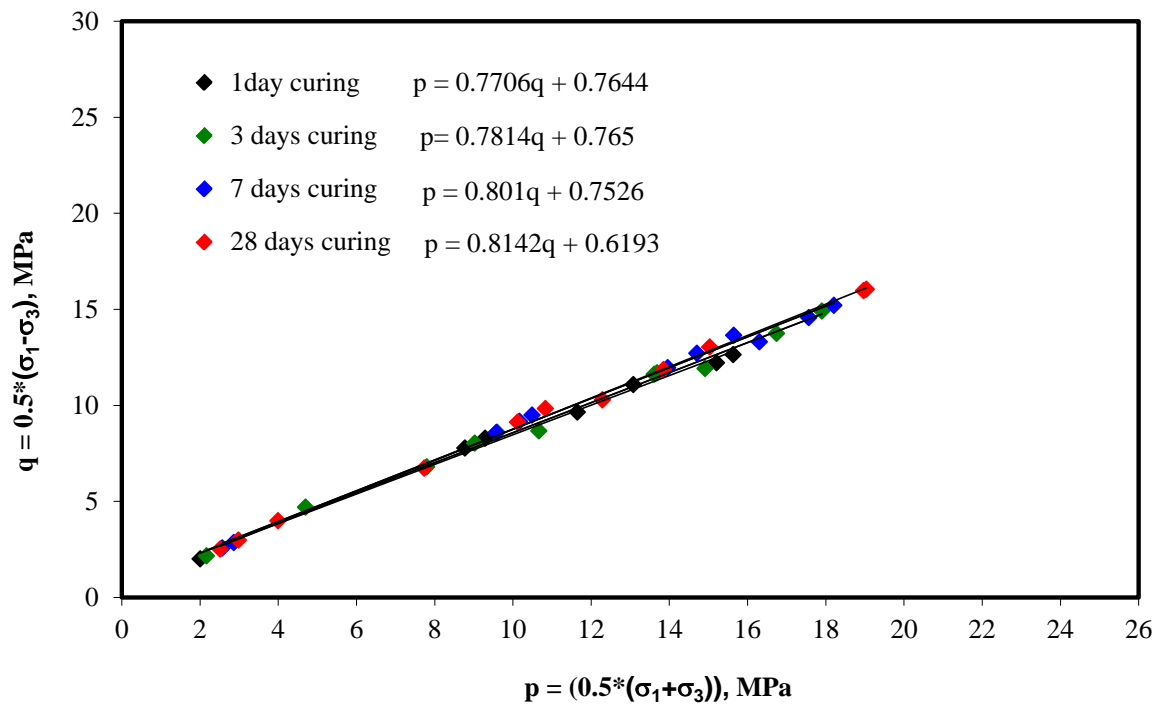
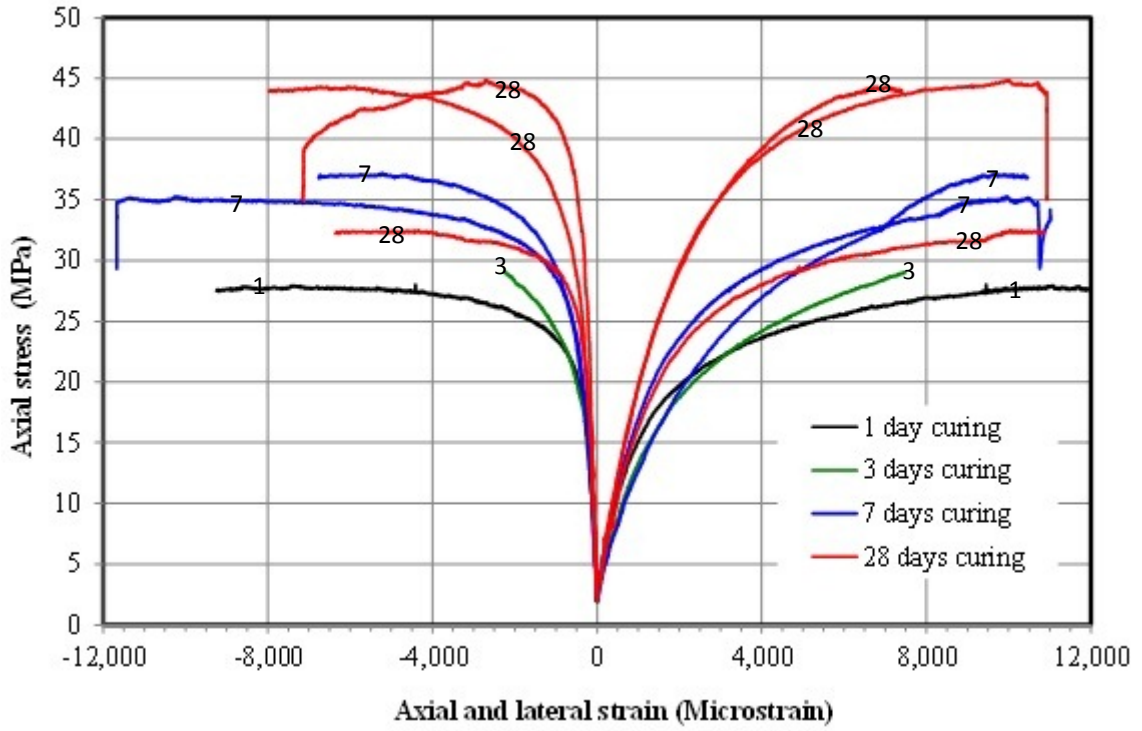Figure 6. Residual shear strength envelopes plotted on the p-q plane.

Figure 7. Axial stress versus strain curves at 3 MPa confinement.
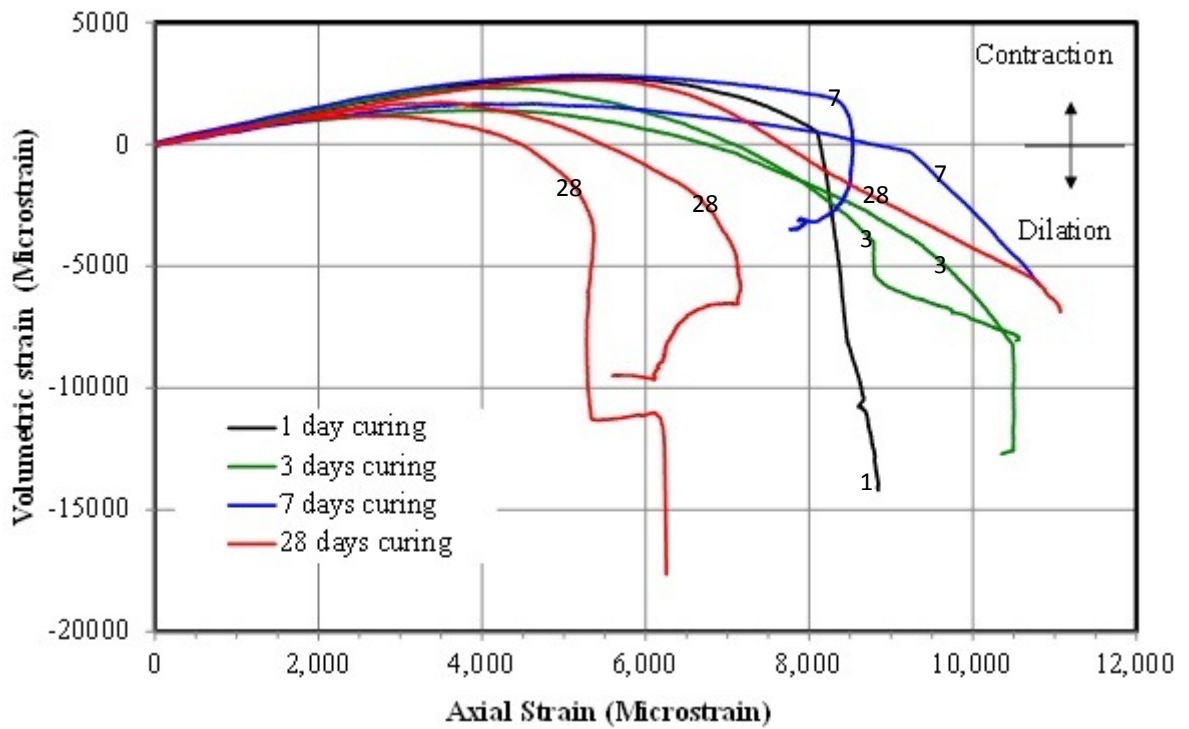

Figure 8. Axial strain versus volumetric versus curves from at 1 MPa confinement.
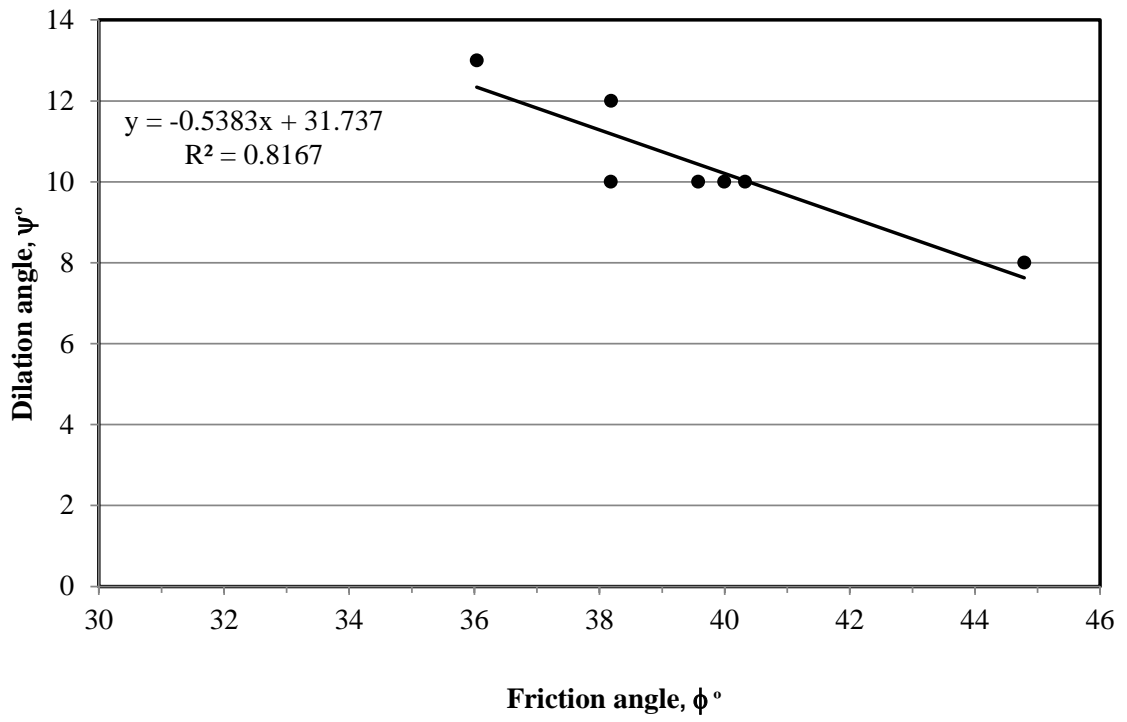
$$y = -0.5383x + 31.737$$
$$R^2 = 0.8167$$

Figure 9. Correlation between the friction angle and the dilation angle.